2021 43rd Annual International Conference of the
IEEE Engineering in Medicine & Biology Society (EMBC)
Oct 31 - Nov 4, 2021. Virtual Conference

High Resolution U-Net for Quantitatively Analyzing Early Spatial Patterning of Human Induced Pluripotent Stem Cells on Micropatterns

Slo-Li Chu, Kuniya Abe, Hideo Yokota, Dooseon Cho, Yuan-Hao Chen,
and Ming-Dar Tsai, Member, IEEE

Abstract— **Human induced pluripotent stem cells (hiPSCs) can differentiate into three germ layer cells, i.e. ectoderm, mesoderm and endoderm, on micropatterned chips in highly synchronous and reproducible manners. The cells are confined within the chip, expanding two-dimensionally as almost in the form of monolayer, thus to be ideal for serving quantitative analysis of their pluripotency. We present a new U-Net (MP-UNet) structure for cell segmentation of early spatial patterning of hiPSCs on micropattern chips using Hoechst fluorescence images. In this structure, the encoding/decoding layers can be dynamically adjusted to extract sufficient image features and be flexible to image sizes. Dice and weight loss functions are designed to identify slight difference in low signal-to-noise ratio, high boundary-to-area ratio and compacted cell images. Several sizes of Hoechst images were tested to show MP-UNet can achieve high accuracy in cell regions and number counting for various sizes of micropattern chips, thus to be excellent quantitative tool for early spatial patterning of hiPSCs.**

I. Introduction

Human induced pluripotent stem cells (hiPSCs) represent an ideal source for patient specific cell-based regenerative medicine. For the clinical use of hiPSCs [1, 2], quality control (QC) of the cell lines will be extremely important. Also, pluripotency of the hiPSCs should be evaluated before use. Embryoid body formation combined with expression analysis has been used for pluripotency test [3], assessing the potential of three germ layers (ectoderm, mesoderm and endoderm and their descendants) formation in vitro. However, it requires relatively long time and the results are not reproducible and quantitative. On the other hand, the micropattern differentiation system can offer rapid, reproducible and quantitative method for pluripotency testing. It has been shown that human embryonic stem cells (hESCs) can generate embryonic spatial patterns, resemblance to the one in the gastrulating human embryos consist of three germ layers [4, 5]. Cells are confined within the chip, expanding two-dimensionally as almost in the form of monolayer, which are ideal for quantitative imaging analysis. The hiPSCs were also confirmed self-organizing on the chips with highly reproducible and synchronous manners [6, 7].

Pluripotent stem cells differentiated on the micropattern chips were stained with antibodies against lineage markers such as SOX2, BRACHYURY, SOX17, and CDX2 for ectoderm, mesoderm, endoderm, and extra-embryonic trophoblast, respectively. DAPI, the nuclei staining reagent, is frequently used to stain cell nuclei for counting number of cells. However, DAPI segmented cell regions were usually smaller than true cell regions and DAPI stain is rather toxic, and not suitable for live cell imaging. In this study, we instead use Hoechst staining for cell segmentation. However, early spatial patterning of hiPSCs on Hoechst fluorescence images usually shows compacted, low signal-to-noise and boundary-to-area ratios. Current image processing and machine learning methods, such as U-Net [8, 9] that was considered an excellent in object segmentation, cannot accurately segment for hiPSCs on Hoechst fluorescence images.

In this paper, we propose a new U-Net (MP-UNet) structure for cell segmentation of early spatial patterning of hiPSCs on micropatterns using the Hoechst microscopy images. Encoding/decoding layer stacks have been adjusted to dynamically accommodate various sizes of images and extract more image features. Dice and weight loss functions are designed to identify slight difference in low signal-to-noise ratio, high boundary-to-area ratio and compacted cell images. Various sizes of Hoechst fluorescence images were tested and high classification accuracies in measuring cell regions and counting the cell number (both better than 87%) were achieved. Thus, the new U-Net structure is effective in segmenting cells and flexible enough to handle various sizes of micropattern chips. The segmented cells on the Hoechst images are then mapped onto SOX2 and BRACHYURY fluorescence images to show the SOX2 or BRACHYURY positive cells with various levels of fluorescence intensities.

II. Materials and Method

A. Cell culture for early spatial patterning of hiPSCs

Human iPS cell line used in this study is 201B7 (HPS0063) and was obtained from RIKEN BioResource Research Center. The iPS cells were cultured and induced to differentiate on the micropattern chip (CYTOO chips, ArenaA 500 μm, 1000 μm, CYTOO Inc. France.) as described in [4].

* Research supported by Ministry of Science and Technology (MOST), R.O.C., under Grant No. 109-2221-E-033-034, 108-2923-E-033-002-MY2, and by RIKEN Presidential Fund: Technology development for quantitative evaluation of cellular state based on image processing and machine learning.

Slo-Li Chu and Ming-Dar Tsai are with Department of Information and Computer Engineering, Chung-Yuan Christian University, Taoyuan, 32023, Taiwan (e-mail: slchu@cycu.edu.tw, mingdar@cycu.edu.tw. Tsai is the corresponding author, phone: +886-3-2654718, fax: +886-3-2654799).

Kuniya Abe and Dooseon Cho are at BioResource Research Center, RIKEN, 3-1-1 Koyadai, Tsukuba, Ibaraki 305-0074, Japan (e-mail: kuniya.abe@riken.jp, dooseon.cho@riken.jp).

Hideo Yokota is with Center for Advanced Photonics, RIKEN, 2-1 Hirosawa, Wako, Saitama 351-0198, Japan, (e-mail: hyokota@riken.jp).

Yuan-Hao Chen is with Master Program in Department of Information and Computer Engineering, Chung-Yuan Christian University.

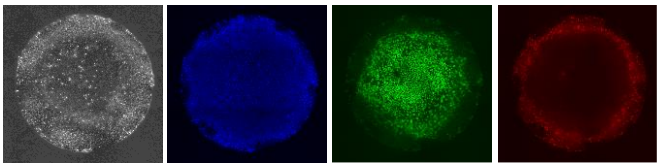

(a) (b) (c) (d)

Figure 1. An example of multi-channel fluorescence microscopy images for hiPS cells in early spatial patterning on a micropattern chip: (a) Bright-field, (b) Hoechst, (c) SOX2, and (d) BRACHYURY.

B. Imaging condition.

Microscopy images of early spatial patterning of hiPSCs were taken by Leica DMI6000B with HC PL FLUOTAR camera. One set of microscopy images in four channels were acquired as shown in Fig. 1. Fig. 1(a) was the bright-field image. Fig. 1(b), 1(c) and 1(d) show fluorescence images of Hoechst, SOX2 and BRACHYURY, respectively, with a pixel resolution of 0.461×0.461μm^2, with resolution of 2560 × 2560 for size of 1000 μm and 1280 × 1280 for 500 μm on the micropatterns.

B. Methods.

1) *MP-UNet network architecture*

Figure 1 shows the proposed MP-UNet architecture that consists of two symmetric parts for extracting cell features: down-sampling and up-sampling parts. Each part consists of variable numbers of layer stacks. Each stack is composed by two layers of convolution and ReLu, together with one Maxpooling layer. These stacks in the down-sampling refines the cell features with particular dimensions to generate corresponding feature maps. Meanwhile, the up-sampling processes the feature map to generate the segmented cell image through the symmetric layer stacks.

The input image including the channel are represented as (*h, w, c*). *h* and *w* indicate the input image size that can be flexible. *c* the channel number, although can be flexible in our system, currently is 1 to indicate one fluorescence color is processed. The input (*x, y, C*) of a specific layer stack in down-sampling is calculated by Eq. 1, where *M* the number of down-sampling/up-sampling layer stacks, *S* the stride of Maxpooling layer to the convolution and ReLu layers

$$(x, y, C) = \left(\frac{h}{S^{i-1}}, \frac{w}{S^{i-1}}, 2^{F+i-1}\right), \quad (1)$$

where *i* indicates the number (from 1 to *M*) of the layer stack, *F* is constant for deciding channels of the layer stacks. *F*, *M*, and *S* are currently set as 5, 6 and 2 obtained during the MP-UNet training according our experiences. Meanwhile, the input of a specific layer stack in up-sampling is symmetric to the ones in the down-sampling as shown in Fig. 1.

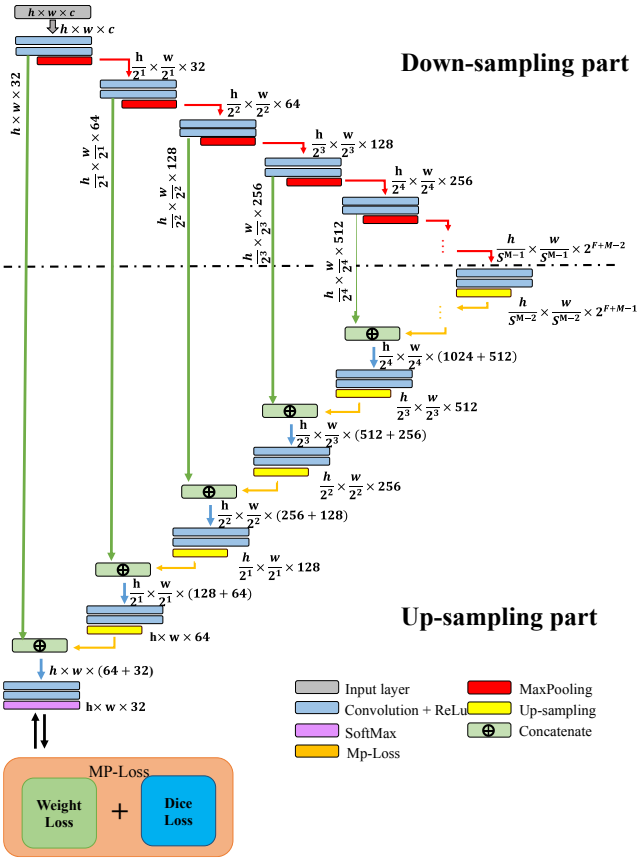

Figure 2. MP-UNet architecture.

2) *Loss function for MP-UNet*

During training, the MP-Loss function, MPL(*X, Y*) is proposed to improve segmenting accuracy for compacted or contacted cells hiPSCs of early spatial patterning on micropatterns. MPL(*X, Y*) is linear combination of a weight loss function *W*(*X, Y*) and a dice loss function *D*(*X, Y*) as Eq. 2. α and β are currently set as 1. $X=[X_1, X_2, \ldots, X_{xy-1}, X_{xy}]$ indicates the pixels of the image predicted by MP-UNet. $Y=[Y_1, Y_2, \ldots, Y_{xy-1}, Y_{xy}]$ indicates pixels of the ground truth image. *W*(*X, Y*), calculated based on cross-entropy function as shown in Eq. 3 and Eq. 4, is used to emphasize some categories. r_k in Eq. 4 indicates the weights of *k* categories, and is used to determine the category importance. For example, the highest value is at the cell boundary. *D*(*X, Y*) can reveal the particular category with larger numbers and reduce the loss value.

$$\mathrm{MPL}(X,Y) = \alpha \times W(X,Y) + \beta \times D(X,Y) \quad (2)$$

$$W(X,Y) = \frac{1}{N}\sum_{j=1}^{N} E(X_j, Y_j) * r_k \quad (3)$$

$$E(X_j, Y_j) = -Y_j \times \log X_j \quad (4)$$

$$D(X,Y) = 1 - 2|X \cap Y|/(|X| + |Y|) \quad (5)$$

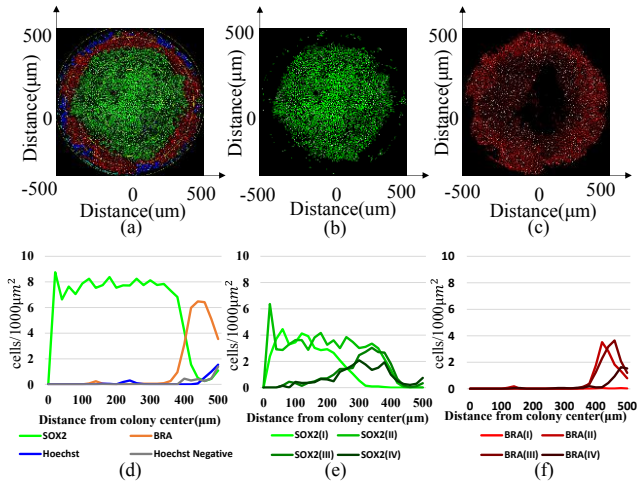

Figure 3. Quantitative analysis of early differentiation stage of hiPSCs cultured on 1000μm micropattern chip

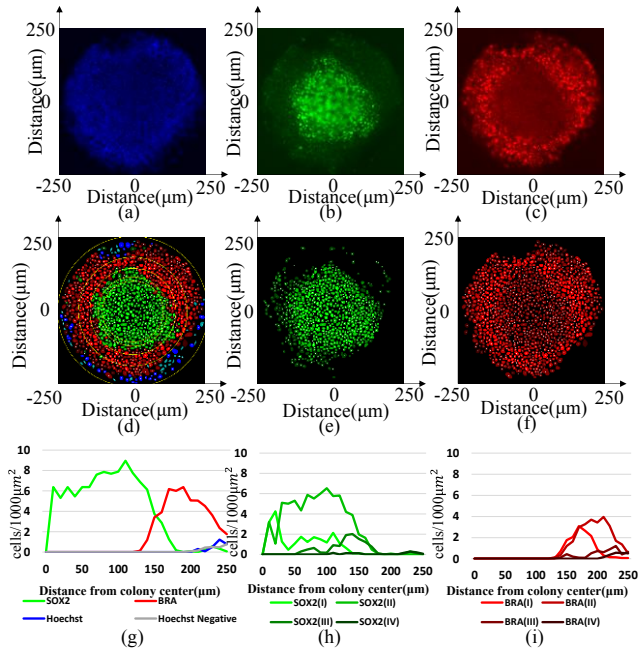

Figure 4. Quantitative analysis of early differentiation stage of hiPSCs cultured on 500μm micropattern chip.

III. Results and Discussion

The MP-UNet was built on a PC with Intel Core i9-9900K 3.60 GHz, 64GB Ram, graphics card of Asus Dual-RTX2080 Ti (11G), and was developed using TensorFlow framework, and Python programming language. Both the convention UNET or proposed MP-UNet were trained two times. First, 1200 (256 × 256 pixels) clipped from mouse ESC nucleus confocal fluorescence images [10] were used to learn the cells with clear image patterns and mild contact. Then, 240 (256 × 256) templates clipped from the Hoechst images were used to further learn the cell features on the Hoechst images. Such size of templates was tested as optimal to learn the cell features on the Hoechst images. The pre-training with another type of cell images were frequently used in machine learning for improving accuracies [11].

A. Quantitative analysis of early differentiation stage of hiPSCs cultured on 1000μm micropattern chip

Figure 3 shown an example of MP-UNet cell segmentation for spatial patterning of hiPSCs on a 1000μm micropattern chip. Fig. 3(a) shows U-net segmented cells on the micropattern chip by processing a Hoechst fluorescence microscopy image as shown in Fig. 1(b). If a Hoechst positive cell corresponds to the ectoderm or mesoderm or others is determined by first mapping the segmented region of this cell to both the SOX2 and BRACHYURY fluorescence images as shown in Fig. 1 (c) and Fig. 1(d). Then, this cell is classified as SOX2 or BRACHYURY positive by comparing the intensities of the mapped region on the SOX2 and BRACHYURY images. That means if it is both SOX2 and BRACHYURY positive, it is assigned to the one with higher intensity. When the cell is both SOX2 and BRACHYURY negative, it is assigned as the Hoechst positive. We also implemented another MP- UNet segmentation for the bright-filed image and found some Hoechst-negative (gray) cells exiting near the outmost part of the micropattern chip. As the result, a cell is assigned as either of the four colors: SOX2 fluorescence (green), BRACHYURY fluorescence (red), and Hoechst fluorescence (blue), and without any fluorescence (gray) as shown in Fig. 3(a). A cell on the SOX2 or BRACHYURY image is further classified as any of four levels according to its intensity on the SOX2 or BRACHYURY image as shown in Fig. 3 (b) and 3(c) that may reveal the cell as some ectoderm or mesoderm subtype.

Fig. 3(d) shows the cell densities of respective types of segmented cells on the micropattern chip. SOX2 positive cells are mainly distributed inside the 300 μm from the center. The BRACHYURY positive cells mainly distributed between 400 μm and 500 μm from the center. The cells of Hoechst positive are also distributed at the outer part of the micropattern chip. However, some Hoechst negative (very weak fluorescence responses) cells were also located at the outer part. A SOX2 or BRACHYURY cell is further classified is any of four subtypes depending on its intensity. Fig. 3(e) and 3(f) shows the SOX2 and BRACHYURY positive cell numbers as in Fig. 3(d) are further divided into four respective subtypes depending on their intensities in the SOX2 and BRACHYURY fluorescence images.

B. Quantitative analysis of early differentiation stage of hiPSCs cultured on 500μm micropattern chip

Figure 4 shows the example of cell segmentation for spatial patterning of hiPSCs on a 500 μm micropattern chip. Fig. 4 (a), (b) and (c) are the original Hoechst, SOX2, and BRACHYURY fluorescence images, respectively. Fig. 4(d) shows the MP-UNet segmented hiPSCs on the chip by processing the Hoechst image as shown in Fig. 4 (a). A segmented cell is assigned as either of the SOX2 (green), BRACHYURY (red), and Hoechst fluorescence (blue). Other (gray) cells are located on the outmost part of the micropattern chip obtained from another MP-UNet segmentation by processing their bright-filed image ((Fig. 4(a)). Figure 4 (e)

and 4(f) show the segmented cells assigned by SOX2 or BRACHYURY fluorescence, where each cell is assigned as any of four levels by its intensity in Fig. 4(b) or Fig. 4(c).

Fig. 4(g) shows the cell density on the micropattern chip. SOX2 positive cells are mainly distributed inside the 150 μm from the center. The BRACHYURY positive cells mainly distributed between 150 μm and 250 μm from the center. The cells with SOX2 and BRACHYURY positive negative but Hoechst positive are distributed at the outer part of the micropattern chip; meanwhile, some Hoechst negative cells (gray) appear at the outer part. Fig. 4(h) and 4(i) shows the SOX2 and BRACHYURY positive cell numbers as in Fig. 4(g) are further divided into four subtypes depending on their intensities in the original fluorescence images.

C. The accuracy evaluation for segmented cell numbers and regions

A Hoechst image (2560 × 2560), and its four, 16, 25 and 64 divisions were used as input images to show the flexibility of the trained MP-UNet. The classified cell numbers for these images are 6098, 6011, 6015, 6027, and 6061, respectively. Comparing to the manual ground-truth number 6915, the accuracy (over 87%) are almost the same for all the image sizes, indicating the trained MP-UNet can achieve the almost same accuracy for any image size, e.g., 1000, 500 and 250 μm of micropatterns. Conversely, the classified numbers by the trained conventional U-net were 532, 2016, 4517, 5196, and 4285, respectively. The suitable input image size is 512 × 512 (25 divisions) where the accuracy achieved 75% that is apparently worse than by MP-UNet. Fig. 5(a) shows the overlap of the segmented cells by MP-UNet with the whole image. Fig. 5(a) shows the overlap of the segmented cells by conventional U-Net with the 25 divisions of the whole image. Fig. 5(c) and 5(e) show a zoom-in of one ROI on the Fig. 5(a) and Fig. 5(b), respectively. Fig. 5(d) shows the same ROI zoom-in but by MP-UNet with the 25 divisions. The white, blue and red regions in these figures are TP (True Positive), FN (False Negative) and FP (False Positive). The region accuracy achieved about 90% for all the figures. But, other sizes by conventional U-net achieved worse accuracy, e.g., 73% for the whole image. The cell connections between divided images classified by MP-Unet (Fig. 5(d)) are also apparently better than by conventional U-Net (Fig. 5(e)) that show MP-Unet can classify out more accurate cell shapes.

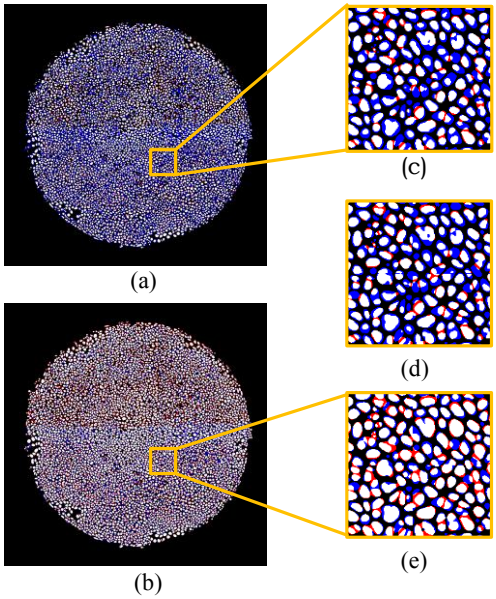

Figure 5. Overlaps of MP-UNet and conventional UNet segmented cells with the original Hoechst fluorescence image.

IV. CONCLUSION

We presented a new U-Net machine learning structure that achieved high accuracies in measuring both the segmented cell number and regions of differentiating hiPSCs from the Hoechst fluorescence microscopy images. The result shows the MP-UNet can achieve novel improvements for the fluorescence images with compacted cells, and low signal-to-noise and boundary-to-area ratios. The future works should accurately classify a segmented cell that mapped onto the fluorescence image as either of the three germ layers and their descendants. The classification of subclasses in the SOX2 and BRACHYURY presented here was based on simple fluorescence intensity. Improved classification should include the effect of image features and pattern of the segmented cell regions.

References

[1] A. Akabayashi, E. Nakazawa, E., and N. S. Jecker, "The world's first clinical trial using iPS cell sheets for corneal epithelial stem cell deficiency," *New Frontiers in Ophthalmology*, vol. 5, pp. 1–2, 2019.

[2] T. Nakajima and M. Ikeya, "Insights into the biology of fibrodysplasia ossificans progressiva using patient-derived induced pluripotent stem cells," *Regenerative Therapy,* vol. 11(1), pp. 125-30, 2019.

[3] A.M. Tsankov, etc., "A qPCR Score Card quantifies the differentiation potential of human pluripotent stem cells", *Nature biotechnology*, vol. 33(11), pp. 1182-1196, 2015.

[4] A. Warmflash, B. Sorre, et al., "A method to recapitulate early embryonic spatial patterning in human embryonic stem cells," Nature Method, vol. 11, pp. 847–854, 2014.

[5] A. Deglincerti, F. Etoc, et al., "Self-organization of human embryonic stem cells on micropatterns," *Nature Protocols,* vo.11, pp. 2223-2232, 2016.

[6] S. Kusuma, Q. Smith, A. Facklam, and S. Gerecht, "Micropattern size-dependent endothelial differentiation from a human induced pluripotent stem cell line," *J Tissue Eng Regen Med.* vol.11(3), pp. 855-861, 2017.

[7] Q. Smith, E. Stukalin, S. Kusuma, S. Gerecht and S. X. Sun, "Stochasticity and Spatial Interaction Govern Stem Cell Differentiation Dynamics", *Scientific Reports*, vol. 5:12617, 2015.

[8] O. Ronneberger, P. Fischer, and T. Brox, "U-Net: Convolutional Networks for Biomedical Image Segmentation", arXiv: 1505.04597. 2015.

[9] T. Falk, et al. "U-Net – Deep Learning for Cell Counting, Detection, and Morphometry", *Nature Methods*, vol. 16, pp. 67-70, 2019

[10] Y.H. Chang, H. Yokota, K. Abe, M.D. Tasi, S.L. Chu, "Automatic three dimensional segmentation of mouse - embryonic stem cell nuclei by utilizing multiple channels of confocal fluorescence images", *Journal of Microscopy*, vol. 281(1), pp. 57-75, 2021.

[11] K. He, R. Girshick, P. Dollár, "Rethinking ImageNet Pre-training", arXiv: 1811.08883. 2018.